Swarm Level 2 Processing System

Intermediate validation of Swarm Level 2 Core Field Product

SW_OPER_MCO_SHAi2C_20131201T000000_20170101T000000_0201

By: DTU

Date: 2017-04-10

Abstract and Conclusion

The processes and tests applied in the intermediate validation of the MCO_SHAi2C product

SW_OPER_MCO_SHAi2C_20131201T000000_20170101T000000_0201

and the conclusions on the product quality drawn herefrom are described in this document.

This product contains the representation of a model of the magnetic field of Earth's core and its temporal evolution ("MCO" part of product name) using spherical harmonic coefficients ("SHA" part of product name). The model is estimated from Swarm and ground observatory data using the *Comprehensive Inversion* (CI) scheme within the Swarm Level 2 Processing system ("2C" part of product name). Operational Swarm Level 1b data version 0501, covering the period from 2013-12-01 to 2016-12-31 are used for the model estimation and the product is valid over the same period ("20131201T000000_20170101T000000" part of product name). This is version 0201 of the product (last part of product name), i.e. same baseline (02) version as the previous CI product release and this is the first, minor version of the product. The format of the product is described in "Product Specification for L2 Products and Auxiliary Products", doc. no. SW-DS-DTU-GS-0001.

The assessment of the SW_OPER_MCO_SHAi2C_20131201T000000_20170101T000000_0201 product shows very good agreement with recent versions of the CHAOS-6 model, [Finlay, EPS, 2016].

The DTU SIL's opinion is that the MCO_SHAi2C product is validated and is therefore suitable for release.

Table of Contents

Table of Figures

Table of Tables

Abbreviations

Acronym	*Description*
CI	Comprehensive Inversion
CMB	Core-Mantle Boundary
EUL	Euler Angle
L2PS	Level 2 Processing System
MCO	Magnetic Core field
PDGS	Payload Data Ground Segment
SHA	Spherical Harmonic Analysis
SIL	Scientist in the Loop
STR	Star Tracker
TDS	Test Data Set
VAL	Validation
VFM	Vector Field Magnetometer

References

[Finlay, EPS, 2016] *Recent geomagnetic secular variation from Swarm and ground observatories as estimated in the CHAOS-6 geomagnetic field model*; Finlay, Christopher C.; Olsen, Nils; Kotsiaros, Stavros; Gillet, Nicolas; Tøffner-Clausen, Lars (2016), Earth Planets Space, Vol 68, 112. doi: 10.1186/s40623-016-0486-1

[Livermore, NGEO, 2017] *An accelerating high-latitude jet in Earth's core*; Livermore, P.W., Hollerbach, R. and Finlay, C.C. (2017), Nature Geoscience, 10, 62-68, doi:10.1038/ngeo2859

[Sabaka, GRL, 2016] *Extracting Ocean-Generated Tidal Magnetic Signals from Swarm Data through Satellite Gradiometry*; Sabaka, Terence J. ; Tyler, Robert H. ; Olsen, Nils in journal: Geophysical Research Letters (ISSN: 0094-8276) doi: 10.1002/2016GL068180, 2016

1 Intermediate Validation Report of MCO_SHAi2C

1.1 Input data products

The following input data products were used for the estimation of the MCO_SHAi2C core field model

Products	Type	Period	Comment
SW_OPER_Q3D_CI_i2__00000000T000000_99999999T999999_0101	Q-matrix of Earth's (1-D mantle + oceans)	-	Used for computing induced part of ionospheric field
SW_OPER_AUX_OBS_2__20130101T000000_20131231T235959_0109 SW_OPER_AUX_OBS_2__20140101T000000_20141231T235959_0109 SW_OPER_AUX_OBS_2__20150101T000000_20151231T235959_0109 SW_OPER_AUX_OBS_2__20160101T000000_20161231T235959_0109	Observatory hourly mean values	2013-12-01 – 2016-10-31	A total of 143 observatories are included
SW_OPER_AUX_DST_2__19980101T013000_20170103T233000_0001 SW_OPER_AUX_F10_2__19980101T000000_20170101T000000_0001 SW_OPER_AUX_KP__2__19990101T023000_20161215T223000_0001	Indices	As indicated by the file names	
SW_OPER_MAGA_LR_1B_*yyyymmddTh1m1s1_yyyymmddTh2m2s2*_0501 SW_OPER_MAGB_LR_1B_*yyyymmddTh1m1s1_yyyymmddTh2m2s2*_0501 SW_OPER_MAGC_LR_1B_*yyyymmddTh1m1s1_yyyymmddTh2m2s2*_0501	Swarm magnetic data, 1 Hz	2013-12-01 - 2016-12-31	Decimated to 15 second sampling

Table 1-1: Input data products

1.2 Model Parameterization and Data Selection

See Section 2.1.

1.3 Output Products

The products of this validation report are:

Swarm Level 2 Magnetic core field Product:

SW_OPER_MCO_SHAi2C_20131201T000000_20170101T000000_0201

Swarm Level 2 Intermediate Validation Product:

SW_OPER_MCO_VALi2C_20131201T000000_20170101T000000_0201

1.4 Validation Results

The tests were conducted between 2017-02-14 and 2017-03-02.

The following tests have been applied to the core field output product. See Annex A for general definitions of various tests.

1.4.1 Spectral Power Density

Figure 1-1 below shows the spectral power density of the static core field model (solid lines for three different epochs) and of the power of the difference between the CI core field model and the CHAOS-6 (dashed lines).

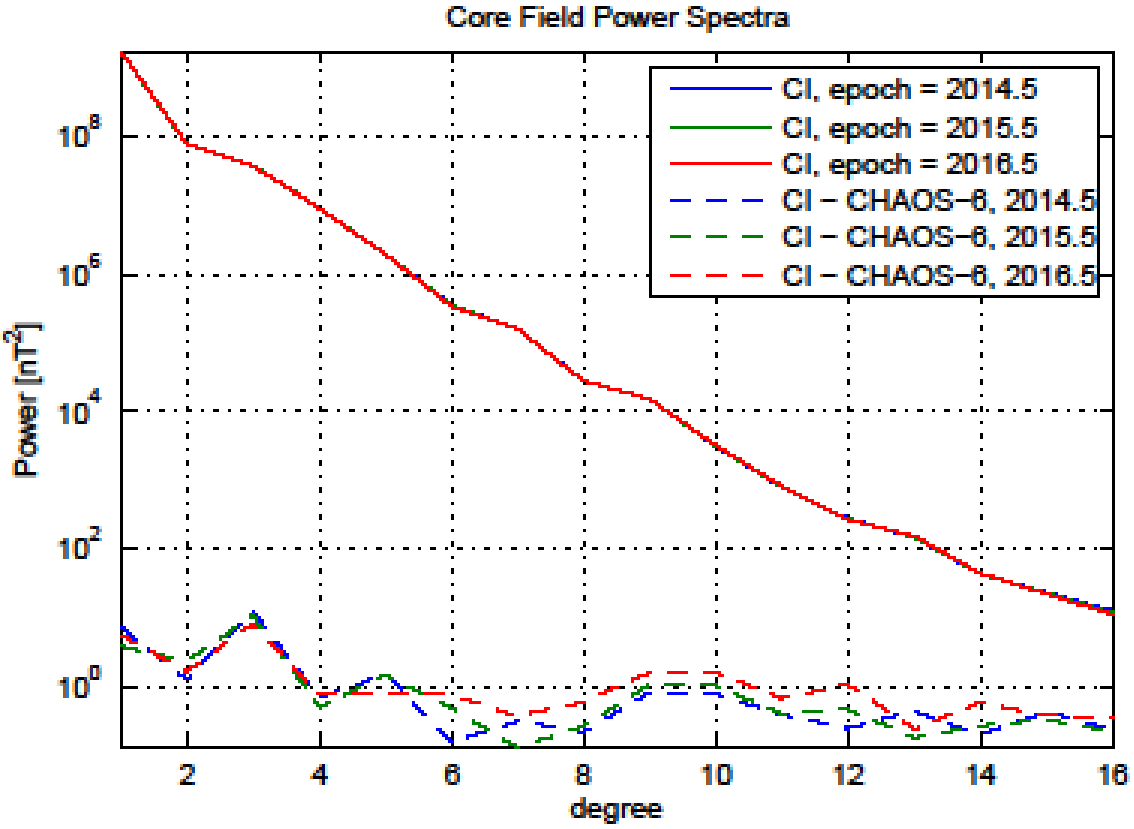

Figure 1-1: Spectral power density, static core field

In Figure 1-2 on the next page are shown the corresponding spectral power density of the first time derivate – the Secular Variation, SV – of the CI model at the three epochs, plus the spectral power of the difference between the CI and CHAOS-6 models.

These plots demonstrate the excellent agreement between the CI core field product and the CHAOS-6 field model.

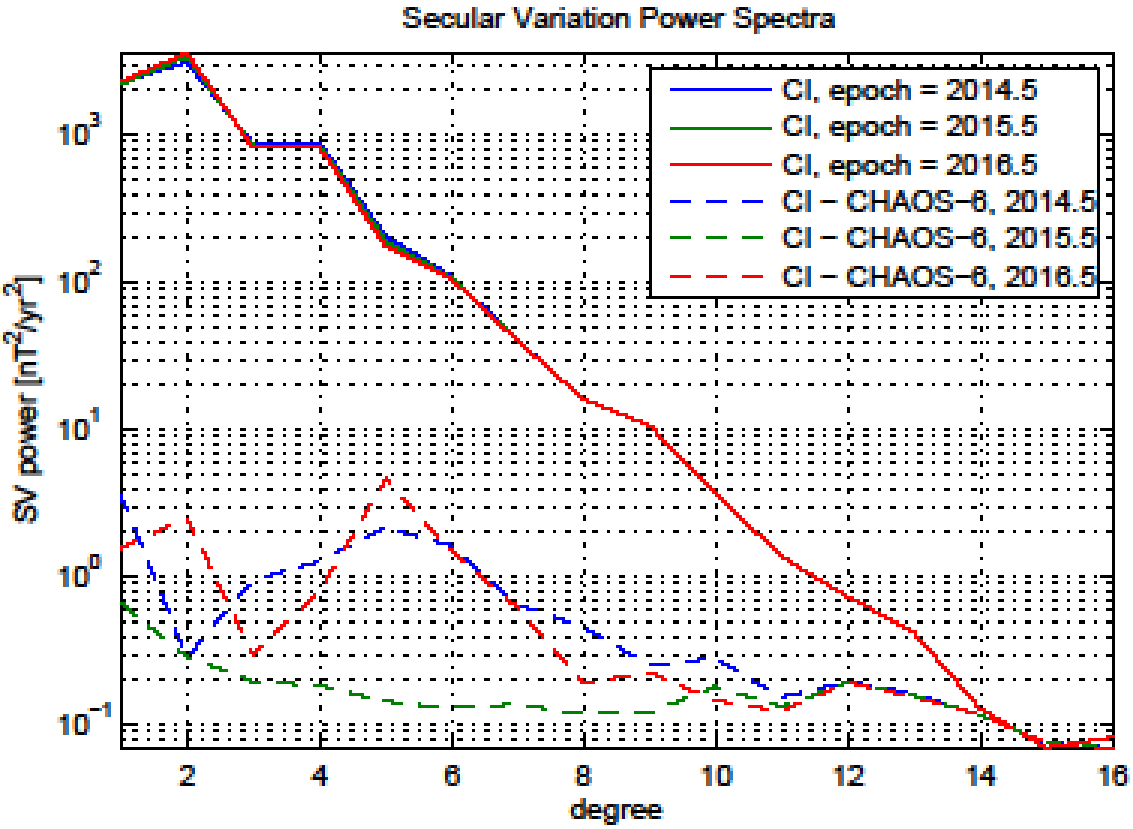

Figure 1-2: Spectral power density, secular variation

1.4.2 Secular Variation per spherical harmonic coefficient

Figure 1-3 below shows timeseries of the first time-derivatives of the spherical harmonic coefficients up to degree 4. The blue curves show the CI core field model coefficient derivatives and the dashed black curves show the CHAOS-6 model coefficient derivatives. The figure confirms the good agreement between the two models.

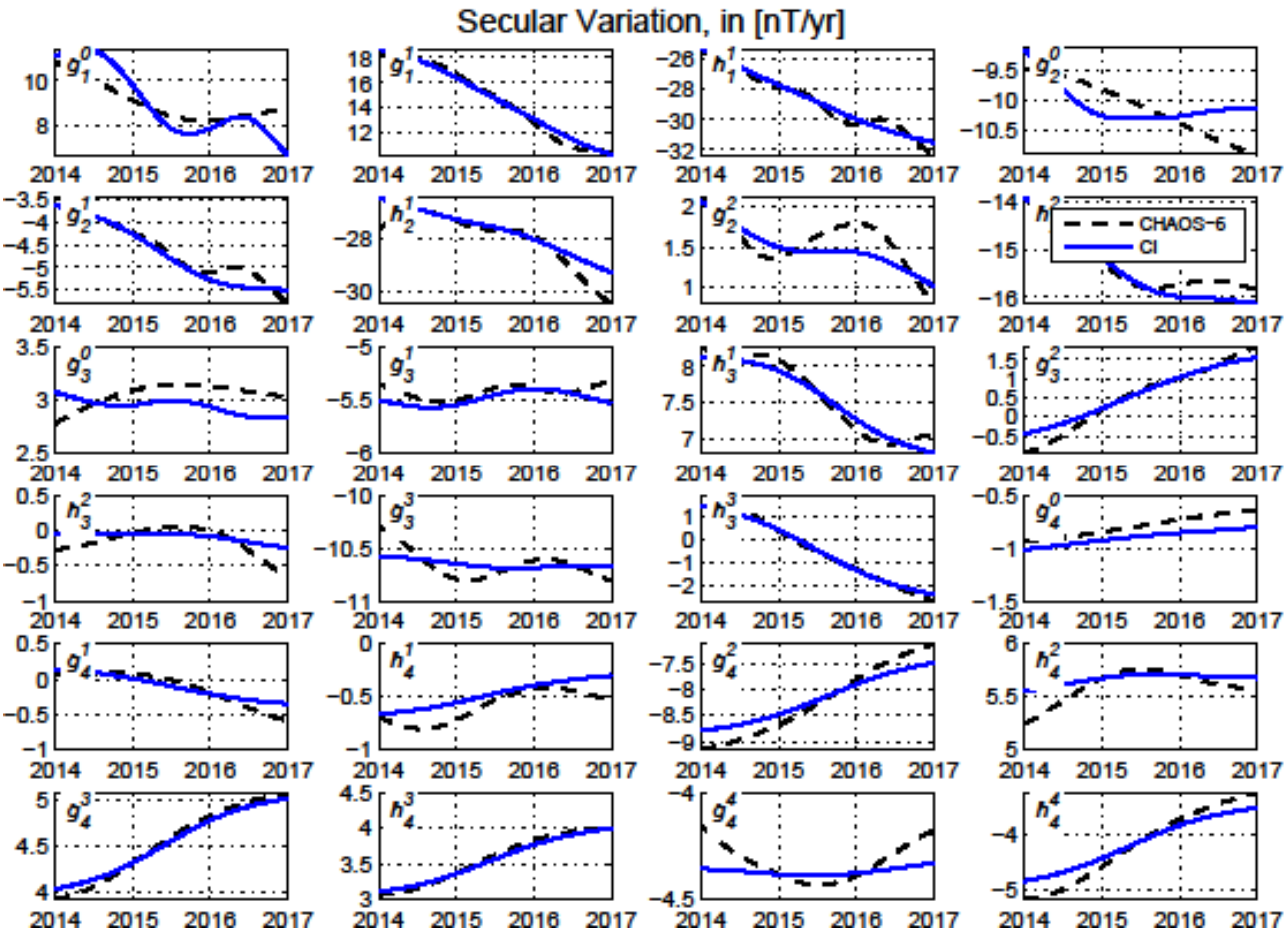

Figure 1-3: Spherical harmonic coefficients, degrees 1-4

1.4.3 Secular Variation at Core-Mantle Boundary

Examining the vertical component of the magnetic field at the core-mantle boundary (CMB) show features similar to those found in CHAOS-6, [Livermore, NGEO, 2017]. Figure 1-4 below shows the first time-derivative of B_r at the CMB at epoch 2015; the large patches in the northern hemisphere (top left) are similar to those in CHAOS-6 whereas the patches in the southern hemisphere (top right) are significantly stronger than those observed in CHAOS-6.

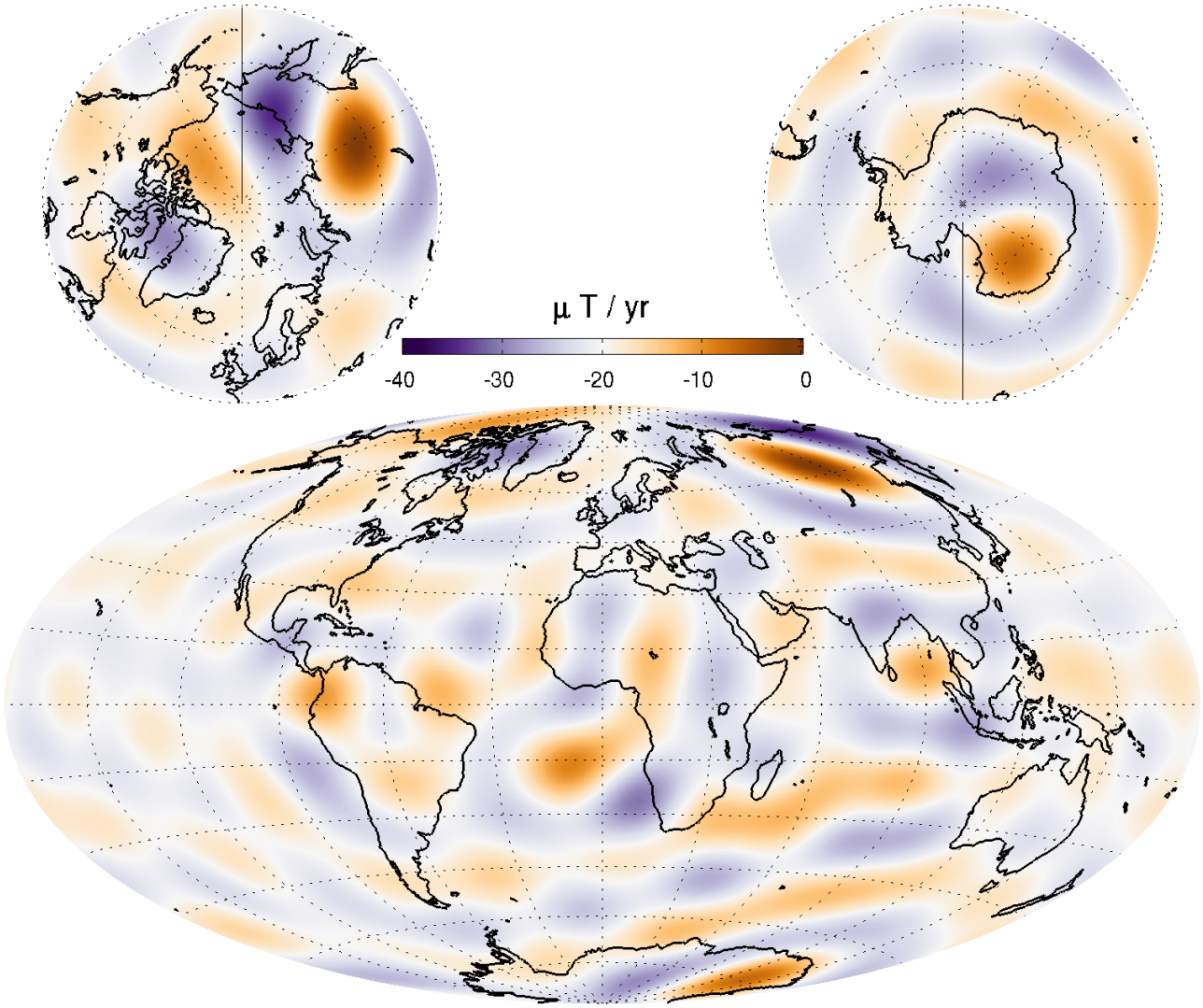

Figure 1-4 Map of dB_r/dt at core-mantle boundary, up to degrees 13, epoch 2015.0

However, looking at the acceleration of B_r, cf. Figure 1-5, the drift of the patches are seen to be very moderate in the CI model.

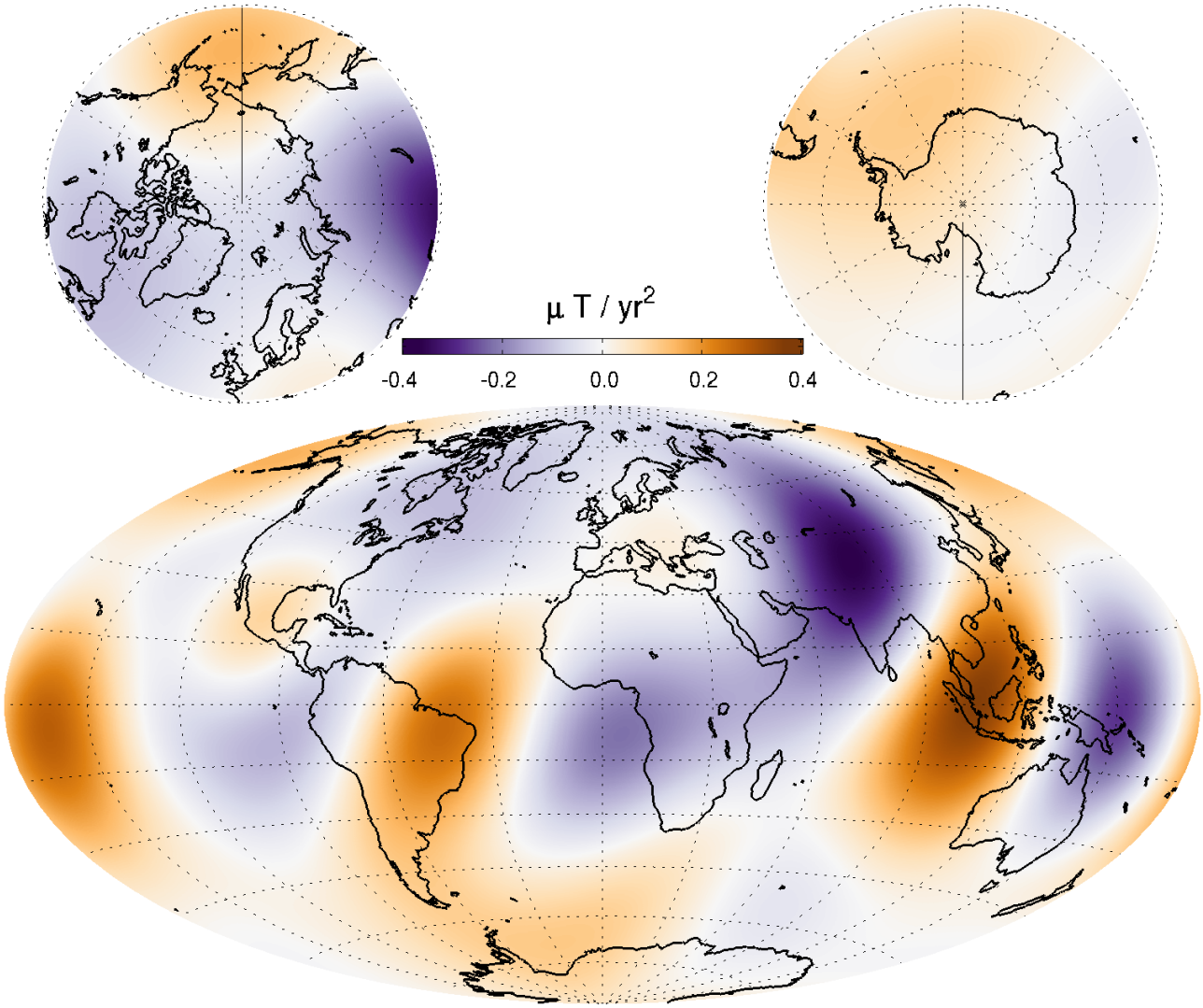

Figure 1-5 Map of d^2B_r/dt^2 at core-mantle boundary, up to degrees 13, epoch 2015.0

1.4.4 Data Statistics

The statistics of the measurement data obtained by the CI modelling are given in Table 1-2 below. Grey cells indicate data from eclipse, white cells indicate data from sunlit regions. Crossed cells indicate data which are not used in the inversion process. “Field” indicate the pure vector and scalar measurements, whereas “NS diff” and “EW diff” indicate the North-South (along-track) respectively East-West differences (“gradients”). The standard deviations (of the residuals between the observations and the estimated model) of the differences are quite impressive; the standard deviations of the direct field measurements from the satellites are also quite excellent whereas the ground observatories show slightly higher residuals than previously recorded. Note also the expected similarity between Swarm A and C (side-by-side flying pair) and North-South differences for all three satellites. Swarm B shows slightly higher residuals in the Field components at low and mid latitudes and slightly lower residuals at high latitudes likely due to its higher altitude.

Swarm/Obs.		Geomagnetic quasi-dipole latitude											
		Low, ≤ 10°				Mid,]10°..55°]				High, > 55°			
		Standard deviations of data residuals, weighted, [nT]											
		$\sigma(B_r)$	$\sigma(B_\theta)$	$\sigma(B_\varphi)$	$\sigma(F)$	$\sigma(B_r)$	$\sigma(B_\theta)$	$\sigma(B_\varphi)$	$\sigma(F)$	$\sigma(B_r)$	$\sigma(B_\theta)$	$\sigma(B_\varphi)$	$\sigma(F)$
A	Field	1.77	3.30	1.98	3.21	2.73	3.62	2.86	2.06				5.97
	NS diff	0.38	0.18	0.37	0.19	0.26	0.33	0.39	0.20				1.84
		1.30	0.98	1.20	0.85	0.61	0.72	1.27	0.33				2.59
B	Field	1.95	4.07	2.84	4.00	3.14	4.48	3.77	2.71				5.78
	NS diff	0.38	0.18	0.36	0.19	0.26	0.34	0.40	0.22				1.61
		1.10	0.79	1.06	0.66	0.58	0.68	1.21	0.31				2.28
C	Field	1.78	3.33	2.02	3.27	2.79	3.66	2.83	2.11				5.98
	NS diff	0.40	0.19	0.38	0.19	0.28	0.35	0.41	0.21				1.85
		1.30	0.98	1.21	0.89	0.63	0.74	1.29	0.33				2.59
A-C	EW diff	0.83	0.36	0.99	0.29	0.43	0.49	0.94	0.28				0.62
		2.10	0.78	2.52	0.55	0.96	1.10	1.64	0.44				0.75
Magnetic observatories		5.70	5.32	4.43	4.81	5.55	5.14	4.44	4.79	16.82	14.01	10.53	17.61
		12.38	13.02	10.88	11.79	8.32	8.93	10.15	8.39	23.42	22.58	16.94	26.04

Table 1-2: Observation Statistics

1.5 Criteria

Table 1-3 below summarizes the criteria used to check the validity of the MCO_SHAi2C product.

Input	Test	Criteria	Pass?
Observations	Residual statistics	Standard deviation of vector data below 7 nT.	Ok
Alternative model	Comparison with model	CI model agrees with alternative model	Ok

Table 1-3: Validation criteria

2 Additional Information

2.1 Model Configuration and Data Selection Parameters

The MCO_SHAi2C product is obtained as a comprehensive co-estimation of the core, lithosphere, ionosphere, and magnetosphere field contributions including induced contributions similar to the method described in [Sabaka, GRL, 2016]. The complete model configuration used is given in Table 2-1 below; the MCO_SHAi2C product is the green part:

Model Part	**Maximum Degree/Order**	**Temporal Characteristics**	**Comment**
Core	16/16	Order 5 B-spline with knots every 6 months	Damping of the mean-square, second and third time derivatives of B_r at the core-mantle boundary (at 3480 km radius).
Lithosphere	90/90	Static	Degree 17-90 purely determined by North-South differences from all satellites and East-West differences of lower pair satellite (A and C). Damping of B_r at the poles to reduce potential effect of lack of data at the poles ("*polar gap*")
Ionosphere	45/5 (dipole coordinates)	Annual, semi-annual, 24-, 12-, 8- and 6- hours periodicity	Spherical harmonic expansion in quasi-dipole (QD) frame, underlying dipole SH $n_{max} = 60$, $m_{max} = 12$. Scaling by 3-months averages of F10.7 plus induction via a priori 3-D conductivity model ("1-D + oceans") and infinite conductor at depth. Damping of: 1. Mean-square current density J in the E-region within the nightside sector (magnetic local times 21:00 through 05:00) 2. Mean-square of the surface Laplacian of J multiplied by a factor of $\sin^8(2\theta)$ over all local times, where θ is co-latitude.

Model Part	Maximum Degree/Order	Temporal Characteristics	Comment
Magnetosphere, external	3/1	One hour bins	
Magnetosphere, induced	3/3	One hour bins	
M2 Tidal	36/36	Periodicity: 12.42060122 hr, phase fixed with respect to 00:00:00, 1999 January 1 GMT	

Table 2-1: Model Configuration

The data selection criteria are:

- Coarse agreement with CHAOS-6 field model: $\Delta B_c \leq 500$ nT for all components $c=r,\vartheta,\varphi$, and $\Delta F \leq 100$ nT.
- $Kp \leq 3^0$
- Time-derivative of Dst: $|dDst/dt| \leq 3$ nT/hour
- 15 second satellite sampling period
- core and tidal fields determined from night-side data only, i.e. with Sun $\geq 10°$ below the horizon

2.2 Comments from Scientists in the Loop

2.2.1 Derivation of Model

The final Comprehensive Inversion model using three years of Swarm data shows good agreement with alternative model and very good statistics (Table 1-2), although some caution must be taken when studying some features at the core-mantle boundary (Section 1.4.3).

2.2.2 Conclusion

The estimated model is assessed to be of good quality with well-behaved characteristics and very good agreement with alternative core field model.

Annex A Definitions of Tests

A.1 Mean square vector field difference per spherical harmonic degree

The mean square vector field difference between models per spherical harmonic degree (n) is diagnostic of how closely the models match on average across the globe. The difference between Gauss coefficients ${}_{}g_n^m$ of model i and model j can be defined as:

$$ {}_{i,j}R_n = (n+1)\left(\frac{a}{r}\right)^{(2n+4)} \sum_{m=0}^{n}\left[{}_i g_n^m - {}_j g_n^m\right]^2 $$

Equation A-1

where n is the degree, m is the order, a is the magnetic reference spherical radius of 6371.2 km which is close to the mean Earth radius, and r is the radius of the sphere of interest, which is taken as r = a for comparisons at the Earth's surface and r = 3480 km for comparisons at the core-mantle boundary.

Summing over degrees n from 1 to the truncation degree N and taking the square root yields the RMS vector field difference between the models i and j averaged over the spherical surface:

$$ {}_{i,j}R = \sqrt{\sum_{n=1}^{N} {}_{i,j}R_n} $$

Equation A-2

A.2 Correlation per spherical harmonic degree

Analysis of spherical harmonic spectra is a powerful way to diagnose differences in amplitude between models but tells us little about how well they are correlated. The correlation per degree between two models again labelled by the indices i and j can be studied as a function of spherical harmonic degree using the quantity: ${}_{i,j}\rho_n$

$$ {}_{i,j}\rho_n = \frac{\sum_{m=0}^{n}\left({}_i g_n^m \; {}_j g_n^m\right)}{\sqrt{\left(\sum_{m=0}^{n}\left({}_i g_n^m\right)^2\right)\left(\sum_{m=0}^{n}\left({}_j g_n^m\right)^2\right)}} $$

Equation A-3

Ideally, the correlation should be close to 1 for all models, indicating that they have equivalent features and coefficients. If the correlation falls below 0.5, for degrees 1-9, then the models should be examined in more detail. Coefficients from degree 10-13 in IGRF and WMM are less well-determined (e.g. due to noise) and also change more rapidly so are not expected to be well correlated by the launch of the Swarm mission.

A.3 Visualisation of coefficient differences

A final method of visualising the differences in Gauss coefficients is to plot the differences ${}_i g_n^m - {}_j g_n^m$ as a triangular plot, with the zonal coefficients lying along the centre of the triangle, the sectorial coefficients along the edges and the tesseral coefficients filling the central regions. These plots will illustrate which, if any, coefficients are strongly divergent between models.